Scientific Paper / Artículo Científico

UNIVERSIDAD POLITÉCNICA SALESIANA ECUADOR
INGENIUS
Revista de Ciencia y Tecnología
https://doi.org/10.17163/ings.n32.2024.04
pISSN: 1390-650X / eISSN: 1390-860X

Radiative heat transfer in H_2O and CO_2 mixtures

Intercambio térmico radiante en mezclas de H_2O y CO_2

Yanan Camaraza-Medina[1,*]

Received: 27-11-2023, Received after review: 07-05-2024, Accepted: 13-05-2024, Published: 01-07-2024

Abstract

This study presents an approximate solution for assessing radiation heat exchange within a gaseous participating medium consisting of H_2O and CO_2 This solution is applicable for values of the product of the total pressure and the mean beam length (PL), ranging from 0.06 to 20 $atm \cdot m$, and temperatures (T) ranging from 300 K to 2100 K. To approximate the exact solutions, the Spence root weighting method is employed. The exact spectral emissivity and absorptivity $\varepsilon\lambda$ and $a\lambda$ of the gas mixture for each set of PL and T values are calculated using the analytical solution (AS). Additionally, the values of the emissivity and absorptivity of the mixture ε_m y a_m are determined using the Hottel graphical method (HGM) and the proposed approximate solution. The HGM shows a weaker correlation, with mean errors of ±15% and ±20% for 54.2% and 75.3% of the evaluated data, respectively. In contrast, the proposed method yields the best fit, with mean errors of ±10% and ±15% for 79.4% and 98.6% of the evaluated data, respectively. In all cases, the agreement between the proposed model and the available experimental data is deemed sufficiently robust to warrant consideration for practical design applications.

Keywords: Participating media, emissivity, absorptivity, view factor, thermal radiation

Resumen

En este trabajo se presenta una solución aproximada para evaluar el intercambio de térmico por radiación a través de un medio participante gaseoso compuesto por H_2O y CO_2, la cual es válida para valores del producto de la presión total y la longitud característica del haz de radiación (PL) desde 0,06 hasta 20 $atm \cdot m$ y temperaturas (T) desde 300 K a 2100 K. Para la aproximación de las SA disponibles es utilizado el método de ponderación de raíces de Spence. Para cada juego de valores PL ;T es calculado el valor de emisividad y absortividad espectral exacta $\varepsilon\lambda$ y $a\lambda$ para la mezcla de gases mediante la solución analítica (SA) y el valor de la emisividad y absortividad de la mezcla ε_m y a_m , usando el método gráfico de Hottel (MGH) y la solución aproximada propuesta. El peor ajuste de correlación se corresponde al MGH, con errores medios de ±15 % y ±20 % para el 54,2 % y 75,3 % de los datos evaluados, respectivamente, mientras que método propuesto proporciona el mejor ajuste, con errores medios de ±10 % y ±15 % para el 79,4 % y 98,6 % de los datos evaluados. En todos los casos, el acuerdo del modelo propuesto con los datos experimentales disponibles es lo suficientemente bueno como para ser considerado satisfactorio para el diseño práctico.

Palabras clave: medios participantes, emisividad, absortividad, factor de visión, radiación térmica

[1,*]Departamento de Ingeniería Mecánica, Universidad de Guanajuato, México.
Corresponding author ✉: ycamaraza1980@yahoo.com.

Suggested citation: Camaraza-Medina, Y. "Radiative heat transfer in H_2O and CO_2 mixtures," *Ingenius, Revista de Ciencia y Tecnología*, N.° 32, pp. 36-47, 2024, DOI: https://doi.org/10.17163/ings.n32.2024.04.

1. Introduction

In the analysis of thermal radiation exchange between surfaces, it is frequentlyassumed for simplicity that both surfaces are separated by a non-participating medium. This assumption implies that the medium neither emits, scatters, nor absorbs radiation. Atmospheric air at common temperatures and pressures approximates a non-participating medium. Gases composed of monoatomic molecules, such as helium and argon, or symmetric diatomic molecules, such as O_2 and N_2, exhibit behavior akin to that ofa non-participating medium, except at extremely high temperatures where ionization occurs. For this reason, in practical radiation calculations, atmospheric air is regarded asa non-participating medium [1–3].

Gases with asymmetric molecules, such as SO_2,CO,H_2O,CO_2, and hydrocarbons C_mH_n, can absorb energy during radiative heat transfer processes at moderate temperatures. At high temperatures, such as those in combustion chambers, they can simultaneously emit and absorb radiation. Hence, in any medium containing these gases at adequate concentrations, the impact of the participating medium must be taken into account inradiation calculations. Combustion gases in a furnace or chamber contain significant quantities of H_2O and CO_2 consequently, the thermal assessment must incorporatethe participating effect of these gases [4, 5].

The presence of a participating medium complicates the analysis of thermal radiation exchange. The participating medium absorbs and emits radiation throughout its volume, rendering gaseous radiation a volumetric phenomenon. This dependency on the size and shape of the body persists even if the temperature is uniform throughout the medium. Solids emit and absorb radiation across the entire spectrum; however, gases emit and absorb energy in multiplenarrow wavelength bands. This suggests that assuming a grey body is not always suitable for gases, even when the surrounding surfaces are grey. The specific absorption and emission properties of gases within a mixture are also contingent on the pressure, temperature, and composition of the mixture. Hence, the radiation characteristics of a particular gas are affected by the presence of other participating gases, stemming from the overlap of emission bands from each component gas in the mixture [6–8].

In a gas, the distance between molecules and their mobility is greater than in solids, allowing a significant portion of radiation emitted from deeper layers to reach the boundary of the mass. Thick layers of gas absorb more energy and transmit less than thin layers. Therefore, in addition to specifying the properties determining the gas state (temperature and pressure), it is also necessary to definea characteristic length L of the gas mass to determine its radiative properties. The emissive and absorptive powers are expressed as a function of this length L through which radiation must travel within the mass. Thus, in gases, the emissive power ε is a function of the product of the gas's partial pressure, denoted as P_x and the characteristic length of the radiation beam L [9–11].

The propagation of radiation through a participating medium can be complex due to the concurrent influence of aerosols, including dust, soot particles (unburnt carbon), liquid droplets, and ice particles, which scatter radiation. Scattering entails alterations in the radiation direction due to reflection, refraction, and diffraction. Rayleigh scattering, induced by gas molecules, typically exerts a minimal impact on heat transfer. Numerous researchers have undertaken advanced investigations into thermal radiation exchange within scattering media [12–14].

The investigation of thermal radiation exchange within participating media has been a research subject for several decades. Among the methodologies commonly employed and endorsed in specialized literature is the Hottel Graphical Method (HGM), renowned for yielding an average deviation of $\pm 25\%$. However, HGM requires reading and interpreting experimental nomograms, introducing additional errors stemming from visual graph interpretation. Consequently, in numerous instances, the actual deviation may surpass $\pm 35\%$, thus posing a notable limitation to its applicability [15, 16].

It initially entails establishing the analytical solution of the view factor, which is succeeded by volumetric integration, a process that can be streamlined by utilizing vector calculus advantages. The mathematical procedure involves managing an extensive array of primitive functions, often necessitating numerical methods to resolve special functions derived from cylindrical or spherical contours (such as Bessel, Spence, and Godunov functions). Consequently, an analytical solution (AS) for this problem category remains elusive, thus prompting reliance on approximate methods, predominantly derived from the Monte Carlo method, alongside numerical techniques and the finite element method [17–19].

While participating media can encompass liquid or semi-transparent solids, such as glass, water, and plastics, this study confines its scope to gases emitting and absorbing radiation. Specifically, the investigation will concentrate on the radiation emission and absorption properties of H_2O and CO_2, given their prevalence as the predominant participating gases in practical applications. Notably, combustion products in furnaces and combustion chambers burning hydrocarbons contain these gases in elevated concentrations [20–22].

The study aims to procure an approximate solution for assessing thermal radiation exchange within a gaseous participating medium comprising H_2O and CO_2. This solution aims to mitigate high mathemati-

cal intricacy while maintaining an acceptable margin of error compared to the analytical solution (within ±15%), suitable for engineering applications. Additionally, this research endeavors to derive analytical solutions to determine the value of L across various geometric configurations of surfaces frequently used in engineering, alongside elucidating the emissivity and absorptivity characteristics of the participating gas mixture.

For comparative analysis, analytical solutions were computed for 355 permutations of thermodynamic temperature within the range 300 $300K \leq T \leq 2100K$, and the product of the total pressure of the gas mixture and the characteristic length of the radiation beam (PL) within the range $0,06\ atm{\cdot}m \leq PL \leq 20\ atm{\cdot}m$. For each PL and T combination, the exact spectral emissivity and absorptivity $\varepsilon\lambda$ y $a\lambda$ for the gas mixture were determined using the analytical solution (AS). In contrast, the emissivity and absorptivity of the mixture ε_m y a_m were evaluated using the Hottel Graphical Method (HGM) and the proposed approximate solution.

Considering the pragmatic nature of the contribution and the favorable adjustment values obtained, the proposed method emerges as a fitting tool for implementation in thermal engineering and allied disciplines necessitating thermal radiation computations through participating media.

2. Materials and Methods

2.1. Radiative Properties in a Participating Medium

Consider a participating medium with a specified thickness. An incident spectral radiation beam of intensity $I_{\lambda(0)}$ impinges upon the medium and undergoes attenuation as it progresses, primarily due to absorption. The decrease in radiation intensity as it traverses a layer of thickness dx is directly proportional to both the intensity itself and the thickness dx. This phenomenon, known as Beer's Law, is mathematically expressed as [23]:

Where k_λ is the spectral absorption coefficient of the medium.

By separating variables in equation (1) and integrating within the limits x=0 to x=L, we obtain [13]:

$$dl_{\lambda(x)} = -k_\lambda I_{\lambda(x)} dx \tag{1}$$

In the derivation of equation (2) an assumption has been made that the absorptivity of the medium remainsindependent of x, based on its exponential decrease. The spectral transmissivity of a medium can be defined as the ratio of the intensity of radiation exiting the medium to that entering it, expressed as:

$$\frac{I_{\lambda(L)}}{I_{\lambda(o)}} = e^{-k_\lambda L} \tag{2}$$

The spectral transmissivity τ_λ of a medium represents the fraction of radiation transmitted through that medium at a specific wavelength. Radiation traversing a non-scattering (and consequently non-reflective) medium is either absorbed or transmitted. Hence, the following relationship holds [12]:

$$\tau_\lambda = \frac{I_{\lambda(L)}}{I_{\lambda(o)}} = e^{-k_\lambda L} \tag{3}$$

$$\alpha_\lambda + \tau_\lambda = 1 \tag{4}$$

By combining equations ((3) and (4) we derive the spectral absorptivity of a medium with thickness L, expressed as equation (5):

$$\alpha_\lambda = 1 - e^{-k_\lambda L} \tag{5}$$

Following Kirchhoff's law, the spectral emissivity is expressed as equation (6):

$$\varepsilon_\lambda = \alpha_\lambda = 1 - e^{-k_\lambda L} \tag{6}$$

Therefore, a medium's spectral absorptivity, transmissivity, and emissivity are dimensionless values equal to or less than one. The coefficients ε_λ, α_λ and τ_λ vary according towavelength, temperature, pressure, and the composition of the mixture [12].

2.2. Mean beam length

The emissivity and absorptivity of a gas depend on the characteristic length, the shape and the size of the gaseous mass involved. In their experiments during the 1930s, Hottel and his colleagues postulated that radiation emission originates from a hemispherical gas mass directed towards a small surface element positioned at the center of the hemisphere's base. Hence, extending the emissivity data of gases examined by Hottel to gas masses with different geometric arrangements proves advantageous. This extension is accomplished by introducing the concept of characteristic or mean beam length L, which represents the radius of an equivalent hemisphere [24–26].

The analytical solution (AS) for deriving the spectral emissivity of the participating gas mixture is a function of the product of the length L, the partial pressure of the participating component, and the view factor between the emitting and receiving surfaces (see Figure 1. This is expressed by the following mathematical relationship (7), [27]:

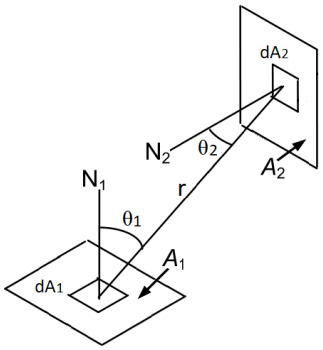

Figure 1. Basic geometry of the view factor

$$\varepsilon_\lambda = \frac{V_{gas}}{\pi A}\int_0^\infty P_P dP \int_0^\infty (1-e^{-k_\lambda L})d\lambda \int_{A_1}\int_{A_2}\frac{cos\theta_1\ cos\theta_2}{r^2}dA_1\ dA_2 \tag{7}$$

Where: A_1 and A_2 are the emitting and receiving surfaces, respectively θ_1,θ_2: are the angles between the normal vector to the areas dA_1 and dA_2 and the line connecting the center of the surfaces A_1 y $A_2 \cdot A, V_{gas}$ represent the total area of the heating surfaces and the volume of the enclosure, respectively. R is the distance between the centers of the surfaces A_1 y A_2.

Equation (7) is very complex for practical engineering calculations, which is why simplifications or approximations are often used [28].

Solving equation (7) is a complex task, largely owing to the multitude of primitive functions and immediate integrals involved in the integration process. Consequently, analytical solutions (AS) for specific cases exist in specialized literature to ascertain the values of L [29]. However, for other prevalent configurations, only experimentally derived approximate values are accessible [30].

2.3. Emissivity and absorptivity of participating gases and their mixtures

The radiative properties (RP) of an opaque solid are independent of its shape or configuration; however, the geometric shape of a gas does impact its RP. The spectral absorptivity of CO_2 consists of four absorption bands located at wavelengths of 1,9 μm, 2, 7μm, 4,3μm and 15μm [31].

The minima and maxima of this distribution and their discontinuities indicate notable distinctions between the absorption bands of a gas and those of a grey body. The width and shape of these absorption bands exhibit variability in response to changes in pressure and temperature. Furthermore, the thickness of the gas layer exerts a significant influence. Hence, accurate estimation of the Radiative Properties (RP) of a gas necessitates the consideration of these three parameters [32].

Absorption and emission in gases exhibit discontinuities across the spectrum. Radiative Properties (RP) are notably pronounced within specific bands at various wavelengths while diminishing towards zero in adjacent bands. The complexity increases in gaseous mixtures due to the overlapping spectral bands of constituent gases. Consequently, this fundamental challenge stems from the absence of analytical solutions for predicting RP [33].

In thermal engineering, a method proposed by Hottel has been widely applied to estimate the RP in gaseous mixtures. This approach entails the separate assessment of each gaseous component within the mixture, followed by adjustments to account for factors such as partial pressure, temperature variations, and the spectral band overlap among mixture constituents [29].

This principle allows for predicting the emissivity or absorptivity of a gas mixture with a maximum deviation of ±25%. However, the Hottel method has the disadvantage of relying on the reading and interpretation of the graphical results, which leads to additional errors. Consequently, the estimated RP values may exhibit an average deviation of ±35% or even higher [34].

The partial pressure Px of each component in a gas mixture is expressedby the following relationship [34]:

$$P_x = P \cdot (\%_x) \tag{8}$$

Where: P is the total pressure of the gas mixture. $\%_c$ is the percentage fraction of each gas in the total composition. Note that 1 $atm = 10^5\ N/m^2$.

Hereafter, the subscripts w and c be employed to denote H_2O and CO_2, respectively. The reduced partial pressures for H_2O and CO_2 are given by:

$$P_{WL} = \frac{P_W \cdot L}{0,3048} \tag{9}$$

$$P_{CL} = \frac{P_C \cdot L}{0,3048} \tag{10}$$

Where: P_W and P_C are the partial pressures of H_2O and CO_2 respectively; L is the characteristic length of the radiation beam.

For a unit pressure of 1 atm, the basic emissivities of H_2O and CO_2 are given by equation (11) and (12):

$$\begin{aligned} e_{W1} = \sqrt{P_{WL}}\left\{\sqrt[4]{T}(0,078-0,003\sqrt[4]{T})-0,41\right\}+ \\ \sqrt[4]{P_{WL}}\left\{\sqrt[4]{T}\cdot(0,032-0,018\sqrt[4]{T})+0,88\right\}+ \\ \sqrt[4]{T}(0,007\sqrt[4]{T}-0,03)-0,24 \end{aligned} \tag{11}$$

$$e_{C1} = \left\{ \sqrt{P_{CL}} \left\{ \sqrt[4]{T} \left(0.024 \sqrt[4]{T} - 0.264 \right) + 0.5 \right\} + \sqrt[4]{P_{CL}} \left\{ \sqrt[4]{T} \left(0.484 - 0.042 \sqrt[4]{T} \right) - 0.0774 \right\} + \sqrt[4]{T} \left(0.158 - 0.019 \sqrt[4]{T} \right) - 0.051 \right\}^4 \tag{12}$$

In equations (11) and (12), the gas temperature T is expressed in K. If $P \neq 1$ atm, then the basic emissivities of H_2O and CO_2 computed using equations (11) and (12) must be corrected. These correction factors are determined by the following relationships:

$$C_W = \left\{ \sqrt[4]{P_{WL}} \cdot (0.137 \sqrt[4]{P_{WL}} - 0.047 \sqrt{P_{WL}} - 0.003) - 0.597 \right\} \cdot \left(\frac{P_W + P}{2} \right)^2 + \left\{ \sqrt[4]{P_{WL}} \cdot (0.685 \sqrt{P_{WL}} - 2.033 \sqrt[4]{P_{WL}} + 0.945) + 1.963 \right\} \cdot \left(\frac{P_W + P}{2} \right) + \sqrt[4]{P_{WL}} (0.982 \sqrt[4]{P_{WL}} - 0.33 \sqrt{P_{WL}} - 0.472) + 0.168 \tag{13}$$

$$C_c = \left\{ \sqrt[4]{P_{CL}} (0,332 - 0,0442 \sqrt[4]{P_{CL}}) - 0,61 \right\} \cdot \sqrt{P} + \left\{ \sqrt[4]{P_{CL}} (0,44 \sqrt[4]{P_{CL}} - 1,993) + 2,862 \right\} \cdot \sqrt[4]{P} + \sqrt[4]{P_{CL}} (1,594 - 0,362 \sqrt[4]{P_{CL}}) - 1,171 \tag{14}$$

Therefore, when $P \neq 1$ atm, the emissivities of H_2O and CO_2 are given by:

$$e_W = e_{W1} \cdot C_W \tag{15}$$

$$e_C = e_{C1} \cdot C_C \tag{16}$$

The emissivities derived from equations (15) and (16) correspond to the respective individual fractions of H_2O and CO_2 within the gas mixture.

To determine the total emissivity, it is necessary to determine a correction coefficient that considers the effect of the overlap of the emission bands. This correction factor depends on the temperature and the partial pressures of H_2O and CO_2. To define the correction factor, two combinations involving the partial pressures are established: the sum of the partial pressures and the deviation of the partial pressures, as determined by the following relationships:

$$P_1 = P_{WL} + P_{CL} \tag{17}$$

$$P_2 = P_W / (P_W + P_C) \tag{18}$$

The correction factor is obtained through the direct integration of equation (17). Due to the complexity of the mathematical process, only the correction factors for three predetermined temperature values will be presented here:T=400 K, T=800 K, and $T \geq 1200$ K. These correction factors are expressed as follows:

$$C_{r(T=400K)} = \left\{ \sqrt[4]{P_1} \cdot \left(1.841 \sqrt[4]{P_1} - 0.807 \sqrt{P_1} - 2.282 \right) + 1.059 \right\} \cdot (P_2)^4 + \left\{ \sqrt[4]{P_1} \cdot \left(3.067 \sqrt{P_1} - 9.259 \sqrt[4]{P_1} + 11.07 \right) - 4.585 \right\} \cdot (P_2)^3 + \left\{ \sqrt[4]{P_1} \cdot \left(11.79 \sqrt[4]{P_1} - 3.491 \sqrt{P_1} - 14.15 \right) + 5.678 \right\} \cdot (P_2)^2 + \left\{ \sqrt[4]{P_1} \cdot \left(1.332 \sqrt{P_1} - 4.685 \sqrt[4]{P_1} + 5.667 \right) - 2.249 \right\} \cdot P_2 \tag{19}$$

$$C_{r(T=800K)} = \left\{ \sqrt[4]{P_1} \cdot \left(3.277 \sqrt{P_1} - 10.46 \sqrt[4]{P_1} + 9.524 \right) - 2.387 \right\} \cdot (P_2)^4 + \left\{ \sqrt[4]{P_1} \cdot \left(22 \sqrt[4]{P_1} - 6.7 \sqrt{P_1} - 21.12 \right) + 5.889 \right\} \cdot (P_2)^3 + \left\{ \sqrt[4]{P_1} \cdot \left(4.237 \sqrt{P_1} - 14.2 \sqrt[4]{P_1} + 14.02 \right) - 4.133 \right\} \cdot (P_2)^2 + \left\{ \sqrt[4]{P_1} \cdot \left(2.91 \sqrt[4]{P_1} - 0.869 \sqrt{P_1} - 2.782 \right) + 0.801 \right\} \cdot P_2 \tag{20}$$

$$\begin{aligned} C_{r(T\geq 1200K)} = & \left\{ \sqrt[4]{P_1} \cdot \left(9.731\sqrt{P_1} - 32.35\sqrt[4]{P_1} + 33.49\right) - 10.83 \right\} \cdot (P_2)^4 \\ & + \left\{ \sqrt[4]{P_1} \cdot \left(63.03\sqrt[4]{P_1} - 18.69\sqrt{P_1} - 66.09\right) + 21.64 \right\} \cdot (P_2)^3 \\ & + \left\{ \sqrt[4]{P_1} \cdot \left(10.49\sqrt{P_1} - 35.51\sqrt[4]{P_1} + 36.98\right) - 12.04 \right\} \cdot (P_2)^2 \\ & + \left\{ \sqrt[4]{P_1} \cdot \left(4.939\sqrt[4]{P_1} - 1.533\sqrt{P_1} - 4.589\right) + 1.335 \right\} \cdot P_2 \end{aligned} \tag{21}$$

For temperature values in the ranges $400K < T < 800K$ and $800K < T < 1200K$, the correction factor $C_{r(T)}$ will be determined through Newton's linear interpolation, using the following relationships:

$$400\,\mathrm{K} < T < 800\,\mathrm{K} \quad C_{r(T)} = C_{r(T=400\,\mathrm{K})} + \frac{C_{r(T=800\,\mathrm{K})} - C_{r(T=400\,\mathrm{K})}}{400} \cdot (T - 400) \tag{22}$$

$$800\,\mathrm{K} < T < 1200\,\mathrm{K} \quad C_{r(T)} = C_{r(T=800\,\mathrm{K})} + \frac{C_{r(T\geq 1200\,\mathrm{K})} - C_{r(T=800\,\mathrm{K})}}{400} \cdot (T - 800) \tag{23}$$

Withthe correction factor $C_{r(T)}$ for the mixture established, the effective emissivity of the mixture, denoted e_m is determined by the following equation:

$$e_m = e_W + e_C - C_{r(T)} \tag{24}$$

To determine the absorptivity of the gases, it is necessary to adjustthe reduced partial pressures, as the reference temperature in this case corresponds to the source (emitter or wall). Consequently, equations (9) and (10) are transformed as follows:

$$P_{WLL} = \frac{P_W \cdot L \cdot T}{0.3048 \cdot T_s} \tag{25}$$

$$P_{CLL} = \frac{P_C \cdot L \cdot T}{0.3048 \cdot T_s} \tag{26}$$

Where: T_s corresponds to the temperatures of the emitting surfaces.

For a unit pressure of 1 atm, the basic absorptivities of H_2O and CO_2 are given by:

$$\begin{aligned} a_{W1} = & \sqrt{P_{WLL}} \left\{ \sqrt[4]{T_s} \left(0.078 - 0.003\sqrt[4]{T_s}\right) - 0.41 \right\} \\ & + \sqrt[4]{P_{WLL}} \left\{ \sqrt[4]{T_s} \cdot \left(0.032 - 0.018\sqrt[4]{T_s}\right) + 0.88 \right\} \\ & + \sqrt[4]{T_s} \left(0.007\sqrt[4]{T_s} - 0.03\right) - 0.24 \end{aligned} \tag{27}$$

$$\begin{aligned} a_{C1} = & \{\sqrt{P_{CLL}} \left\{ \sqrt[4]{T_s} \left(0.024\sqrt[4]{T_s} - 0.264\right) + 0.5 \right\} \\ & + \sqrt[4]{P_{CLL}} \left\{ \sqrt[4]{T_s} \cdot \left(0.484 - 0.042\sqrt[4]{T_s}\right) - 0.774 \right\} \\ & + \sqrt[4]{T_s} \left(0.158 - 0.019\sqrt[4]{T_s}\right) - 0.051\}^4 \end{aligned} \tag{28}$$

In equations (27) and (28), the temperature of the emitting surface T_s is given in K.

If $P \neq 1$ atm, then the basic absorptivity values for H_2O and CO_2 need adjustment by incorporating the correction factors calculated with equations (13) and (14) and a thermodynamic factor that addresses the non-uniformity of the temperature distribution on the emitting surface and within the gas. Mathematically, this is expressed as follows:

$$C_{Wa} = C_W \cdot \left(\frac{T}{T_s}\right)^{0.45} \tag{29}$$

$$C_{Ca} = C_C \cdot \left(\frac{T}{T_s}\right)^{0.65} \tag{30}$$

Therefore, when $P \neq 1$ atm, the absorptivities of H_2O and CO_2 are given by:

$$a_W = a_{W1} \cdot C_{Wa} \tag{31}$$

$$a_C = a_{C1} \cdot C_{Ca} \tag{32}$$

The absorptivities calculated using equations (31) and (32) correspond to the individual gaseous fractions of H_2O and CO_2, respectively.

To calculate the total absorptivity, it is necessary to determine a correction coefficient that considers the effect of the overlap of the absorption bands. This correction factor depends on the sum of the reduced partial pressures of H_2O and CO_2, which is obtained using the following relationship:

$$P_3 = P_{WLL} + P_{CLL} \tag{33}$$

The correction factor is obtained through the direct integration of equation (7). Due to the complexity of this integration process, only the correction factors for three predeterminedtemperature values will be provided here: $T = 400K$,$T = 800K$ and $T \geq 1200K$. These correction factors are expressed as follows:

$$
\begin{aligned}
C_{ra(T=400\,\mathrm{K})} = &\left\{\sqrt[4]{P_3}\cdot\left(1.841\sqrt[4]{P_3}-0.807\sqrt{P_3}-2.282\right)+1.059\right\}\cdot(P_2)^4\\
&+\left\{\sqrt[4]{P_3}\left(3.067\sqrt{P_3}-9.259\sqrt[4]{P_3}+11.07\right)-4.585\right\}\cdot(P_2)^3\\
&+\left\{\sqrt[4]{P_3}\left(11.79\sqrt[4]{P_3}-3.491\sqrt{P_3}-14.15\right)+5.678\right\}\cdot(P_2)^2\\
&+\left\{\sqrt[4]{P_3}\cdot\left(1.332\sqrt{P_3}-4.685\sqrt[4]{P_3}+5.667\right)-2.249\right\}\cdot P_2
\end{aligned}
\tag{34}
$$

$$
\begin{aligned}
C_{ra(T=800\,\mathrm{K})} = &\left\{\sqrt[4]{P_3}\cdot\left(3.277\sqrt{P_3}-10.46\sqrt[4]{P_3}+9.524\right)-2.387\right\}\cdot(P_2)^4\\
&+\left\{\sqrt[4]{P_3}\cdot\left(22\sqrt[4]{P_3}-6.7\sqrt{P_3}-21.12\right)+5.889\right\}\cdot(P_2)^3\\
&+\left\{\sqrt[4]{P_3}\left(4.237\sqrt{P_3}-14.2\sqrt[4]{P_3}+14.02\right)-4.133\right\}\cdot(P_2)^2\\
&+\left\{\sqrt[4]{P_3}\cdot\left(2.91\sqrt[4]{P_3}-0.869\sqrt{P_3}-2.782\right)+0.801\right\}\cdot P_2
\end{aligned}
\tag{35}
$$

$$
\begin{aligned}
C_{ra(T\geq1200\,\mathrm{K})} = &\left\{\sqrt[4]{P_3}\cdot\left(9.731\sqrt{P_3}-32.35\sqrt[4]{P_3}+33.49\right)-10.83\right\}\cdot(P_2)^4\\
&+\left\{\sqrt[4]{P_3}\cdot\left(63.03\sqrt[4]{P_3}-18.69\sqrt{P_3}-66.09\right)+21.64\right\}\cdot(P_2)^3\\
&+\left\{\sqrt[4]{P_3}\cdot\left(10.49\sqrt{P_3}-35.51\sqrt[4]{P_3}+36.98\right)-12.04\right\}\cdot(P_2)^2\\
&+\left\{\sqrt[4]{P_3}\cdot\left(4.939\sqrt[4]{P_1}-1.533\sqrt{P_3}-4.589\right)+1.335\right\}\cdot P_2
\end{aligned}
\tag{36}
$$

In equations (34) to (36) the deviation of partial pressures P_2 is calculated using equation (18). For temperature values in the ranges $400K < T < 800K$ and $800K < T < 1200K$, the correction factor $C_{ra(T)}$ will be determined using Newton's linear interpolation, utilizingthe following relationships:

$$
400\,\mathrm{K} < T < 800\,\mathrm{K} \quad C_{ra}(T) = C_{ra}(T=400\,\mathrm{K}) + \frac{C_{ra}(T=800\,\mathrm{K}) - C_{ra}(T=400\,\mathrm{K})}{400}\cdot(T-400) \tag{37}
$$

$$
800\,\mathrm{K} < T < 1200\,\mathrm{K} \quad C_{ra}(T) = C_{ra}(T=800\,\mathrm{K}) + \frac{C_{ra}(T\geq1200\,\mathrm{K}) - C_{ra}(T=800\,\mathrm{K})}{400}\cdot(T-800) \tag{38}
$$

Given the correction factor $C_{ra(T)}$ of the mixture, the effective absorptivity of the mixture a_m is defined by the following equation:

$$
a_m = a_W + a_C - C_{ra(T)} \tag{39}
$$

3. Results and Discussion

3.1. Validation of the Proposed Model

For the validation of the proposed model, random temperature values in the range $300K \leq T \leq 2100K$ are employed, alongside six predetermined values of the product PL (0.06, 0.6, 3, 5, 10, 20 atm · m), with 55, 55, 45, 55, 45, and 80 data points for each PL interval, respectively. For each combination of PL and T, the exact spectral emissivity ε_λ is determined using the analytical solution (AS), whilethe emissivity of the mixture e_m is calculated using the Hottel Graphical Method (HGM) and equation (24).

In Figure 2, the ratio ε_λ/e_m is correlated with temperature T, adjusted within error bands of ±15% and ±20%, using the e_m values obtained through HGM. In Figure 3, the ratio ε_λ/e_m is correlated with temperature T, adjusted within error bands of ±10% and ±15%, using the e_m values calculated through equation (24).

The percentage deviation (error) is computed relative to the AS and is determined using the following relationship [35]:

$$
D_\% = E_\% = 100\cdot\left(\frac{\varepsilon_\lambda - e_m}{\varepsilon_\lambda}\right) \tag{40}
$$

Figure 2 illustratesthat the HGM yields the poorest fit compared to the AS, with mean errors of ±15% and ±20% for 54.2% and 75.3% of the evaluated (PL; T) points. For the HGM, the optimal fit is achievedfor PL = 3.0, with mean errors of ±15% and ±20% for 63.2% and 84.2% of the evaluated data, respectively, while the least favorable fit is obtained for PL = 10,

with mean errors of ±15% and ±20% for 42.7% and 57.1% of the evaluated data.

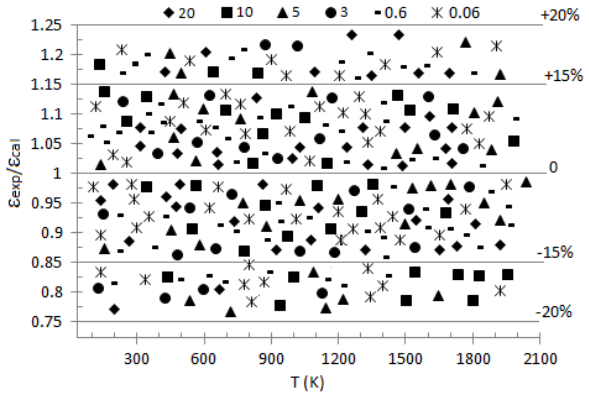

Figure 2. Correlation between temperature T and the ratio ε_λ/e_m using the HGM

Figure 3 illustrates that equation (24) yields superior fitting performance compared to the AS, with mean errors of ±10% and ±15% for 79.4% and 94.9% of the evaluated (PL; T) points. For equation (24), the best fit is obtained for PL = 20, with mean errors of ±10% and ±15% for 83.2% and 98.6% of the evaluated data, respectively . Conversely, the least favorable fitting occurs at PL = 0.6, where mean errors of ±10% and ±15% are registered for 75.1% and 91.9% of the evaluated data.

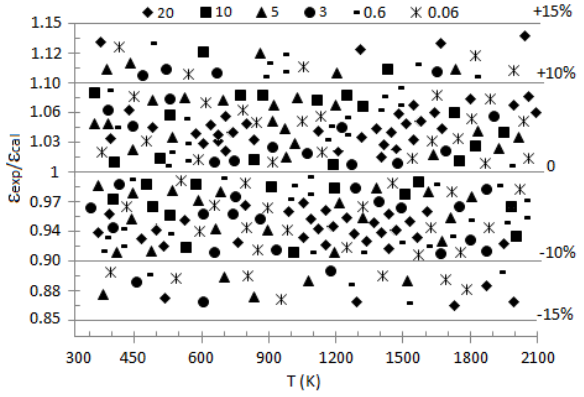

Figure 3. Correlation between temperature T and the ratio ε_λ/e_m using equation (24).

3.2. Application to a Case Study

A pressurized furnace, measuring (length × width × height) 3m × 4m × 5m, contains combustion gases at T=1200K and a pressure P=2 atm In contrast, the surface temperature of the furnace walls, T_S, is maintained at 1100K. Volumetric analysis reveals that the composition of the combustion gases comprises 87% $N2, 8_{\%}$ of H_2O, and 5% of CO_2. The task at hand is to compute the heat transfer between the combustion gases and the furnace walls, consisting of bricks with a grey, satin finish surface.

Using the relationships given in [29], it is determined that $L = 3,04m \approx 3m$. Using equation (8), the partial pressures of H_2O and CO_2 are computed, yielding $P_W = 0,16$ y $P_C = 0,1$, respectively. Subsequently, the reduced partial pressures are determined utilizing equations (9) and (10), resulting in $P_{WL} = 1,575atm \cdot m$ y $P_{CL} = 0,984atm \cdot m$. The fundamental emissivities for H_2O and CO_2 are acquired through equations (11) and (12) correspondingly, yielding $e_{W1} = 0,255$ y $e_{C1} = 0,135$.

Since $P \neq 1atm$, the basic emissivities of H_2O and CO_2 must be corrected using equations (13) and (14), respectively, yielding $C_W = 1,379$ and $C_C = 1$. The actual emissivities of H_2O and CO_2 are determined through equations (15), and (16), resulting in $e_W = 0,3524$ and $e_C = 0,157$. The sum P_1 and deviation P_2 of partial pressures are calculated using relationships (17) and (18), obtaining $P_1 = 2,559atm \cdot m$ and $P_2 = 0,615atm \cdot m$.

The gas mixture temperature is maintained at 1200 K; hence, the correction coefficient $C_{r(T=1200K)}$ is determined utilizing equation (21), resulting in $C_{r(T=1200K)} = 0,052atm \cdot m$. The effective emissivity of the mixture e_m is given by equation (24), resulting in $e_m = 0,458$. Subsequently, employing equation (7) and undergoing a meticulous integration process, the precise value of $\varepsilon_\lambda = 0,463$ is obtained, whereasthe HGM provides a value of $e_m = 0,43$. Using equation (40), the error with respect to the AS is determined, yielding $D_{\%} = 1,08\%$ y $D_{\%} = 7.13\%$, for equation (24) and the HGM, respectively.

The modified reduced pressures are obtained using equations (25) and (26), yielding $P_{WLL} = 1,718atm{\cdot}m$ y $P_{CLL} = 1,073atm \cdot m$. The basic absorptivities for H_2O and CO_2 are calculated using equations (27) and (28) respectively, resulting in $a_{W1} = 0,275$ and $a_{C1} = 0,144$.

Since $P \neq 1atm$, the basic absorptivities of H_2O and CO_2 must be corrected using equations (29) y (30), respectively, yielding $C_{Wa} = 1,434$ and $C_{Ca} = 1,234$ The absorptivities of the fractions of H_2O and CO_2 are determined using equations (31) and (32), resulting in $a_W = 0,394$ and $a_C = 0,178$. The sum of partial pressures P_3 is calculated using equation (33), obtaining $P_3 = 2,791atm \cdot m$.

The temperature of the gas mixture is 1200 K; therefore, the correction coefficient $C_{ra(T=1200K)}$ is estimated using equation (36), $C_{ra(T=1200K)} = 0,053atm{\cdot}m$. The effective absorptivity of the mixture a_m is given by equation (39), resulting in $a_m = 0,519$. Using equations (6) and (7) and undergoing a meticulous handling of immediate integrals, the precise value of $a_{\neq} = 0,525$ is obtained, while the HGM provides a value of $a_m = 0,449$. Using equation (40), the com-

puted error with respect to the AS is determined, yielding $D_{\%} = 1,14\%$ y $D_{\%} = 14,48\%$, for equation (24) and the HGM, respectively.

The furnace walls consist of brick, featuring a grey surface with a satin finish, maintaining an average temperature of $T_S = 1100K$. With these specifications, the surface's normal emissivity is $e_s = 0,75$.

The heat flux exchanged between the gases and the furnace wall is given by:

$$Q_n = \frac{\varepsilon_s + 1}{2} A_s \sigma \left(\varepsilon_m T^4 - a_m (T_s)^4 \right) \qquad (41)$$

The heat flux values exchanged(in kW) are obtained using the AS, the HGM, and equation (24), with the computed error relative to the AS also determined. Table 1 summarizes the obtained heat flux values (in kW) and the corresponding error $E_{\%}$ in each case relative to the AS.

Table 1. Obtained Values Q_n and $E_{\%}$ for the Case Study

Methods	$Q_n(kW)$	$E_{\%}(\%)$
AS	56.822	-
HGM	697.354	–22,4
Proposed method	565.108	0.82

4. Conclusions

Upon comparison with the AS, an approximate method was developed to estimate thermal radiation exchange through participating media. The proposed models were validated by comparing them with the existing AS.

The derived models correlate with all experimental data for both the HGM and the proposed method, exhibiting a mean deviation of ±20% and ±10%, respectively.

For the HGM, the least favorable fitting compared to the AS is achieved for PL=10, exhibiting a mean error of ±20% for 57.1% of the assessed data. In contrast, the optimal fitting occurs for PL=3.0, displaying a mean error of ±15% for 63.2% of the evaluated data. Conversely, for the proposed method, the poorest fitting compared to the AS is observed for PL=0.6, with a mean error of ±15% for 91.9% of the analyzed data. In contrast, the most accurate fitting is achieved for PL=20, with a mean error of ±10% for 83.2% of the evaluated data.

In all instances, the alignment of the proposed model with the available experimental data is sufficiently robust to be deemed satisfactory for practical design purposes.

Acknowledgements

The author extends gratitude for the recommendations provided by Professor Dr. John R. Howell from the Department of Mechanical Engineering at the University of Texas at Austin.

References

[1] M. H. Bordbar, G. Węcel, and T. Hyppänen, "A line by line based weighted sum of gray gases model for inhomogeneous CO_2–H_2O mixture in oxy-fired combustion," *Combustion and Flame*, vol. 161, no. 9, pp. 2435–2445, 2014. [Online]. Available: https://doi.org/10.1016/j.combustflame.2014.03.013

[2] M. F. Modest and R. J. Riazzi, "Assembly of full-spectrum k-distributions from a narrow-band database; effects of mixing gases, gases and nongray absorbing particles, and mixtures with nongray scatterers in nongray enclosures," *Journal of Quantitative Spectroscopy and Radiative Transfer*, vol. 90, no. 2, pp. 169–189, 2005. [Online]. Available: https://doi.org/10.1016/j.jqsrt.2004.03.007

[3] M. Cui, X. Gao, and H. Chen, "Inverse radiation analysis in an absorbing, emitting and non-gray participating medium," *International Journal of Thermal Sciences*, vol. 50, no. 6, pp. 898–905, 2011. [Online]. Available: https://doi.org/10.1016/j.ijthermalsci.2011.01.018

[4] T. J. Moore and M. R. Jones, "Analysis of the conduction–radiation problem in absorbing, emitting, non-gray planar media using an exact method," *International Journal of Heat and Mass Transfer*, vol. 73, pp. 804–809, 2014. [Online]. Available: https://doi.org/10.1016/j.ijheatmasstransfer.2014.02.029

[5] L. J. Dorigon, G. Duciak, R. Brittes, F. Cassol, M. Galarça, and F. H. França, "WSGG correlations based on HITEMP2010 for computation of thermal radiation in non-isothermal, non-homogeneous H_2O/CO_2 mixtures," *International Journal of Heat and Mass Transfer*, vol. 64, pp. 863–873, 2013. [Online]. Available: https://doi.org/10.1016/j.ijheatmasstransfer.2013.05.010

[6] F. Cassol, R. Brittes, F. H. França, and O. A. Ezekoye, "Application of the weighted-sum-of-gray-gases model for media composed of arbitrary concentrations of H_2O, CO_2 and soot," *International Journal of Heat and Mass Transfer*, vol. 79, pp. 796–806, 2014. [Online]. Available: https://doi.org/10.1016/j.ijheatmasstransfer.2014.08.032

[7] F. R. Centeno, R. Brittes, F. H. França, and O. A. Ezekoye, "Evaluation of gas radiation heat transfer in a 2D axisymmetric geometry using the line-by-line integration and WSGG models," *Journal of Quantitative Spectroscopy and Radiative Transfer*, vol. 156, pp. 1–11, 2015. [Online]. Available: https://doi.org/10.1016/j.jqsrt.2015.01.015

[8] Y. Camaraza-Medina, "Polynomial cross-roots application for the exchange of radiant energy between two triangular geometries," *Ingenius, Revista de Ciencia y Tecnoloía*, no. 30, pp. 29–41, 2023. [Online]. Available: https://doi.org/10.17163/ings.n30.2023.03

[9] M. Alberti, R. Weber, and M. Mancini, "Re-creating Hottel's emissivity charts for water vapor and extending them to 40 bar pressure using HITEMP-2010 data base," *Combustion and Flame*, vol. 169, pp. 141–153, 2016. [Online]. Available: https://doi.org/10.1016/j.combustflame.2016.04.013

[10] ——, "Gray gas emissivities for H_2O-CO_2-CO-N_2 mixtures," *Journal of Quantitative Spectroscopy and Radiative Transfer*, vol. 219, pp. 274–291, 2018. [Online]. Available: https://doi.org/10.1016/j.jqsrt.2018.08.008

[11] S. Khivsara, M. U. M. Reddy, K. Reddy, and P. Dutta, "Measurement of radiation heat transfer in supercritical carbon dioxide medium," *Measurement*, vol. 139, pp. 40–48, 2019. [Online]. Available: https://doi.org/10.1016/j.measurement.2019.03.012

[12] M. F. Modest and S. Mazumder, "Chapter 4 - view factors," in *Radiative Heat Transfer (Fourth Edition)*, fourth edition ed., M. F. Modest and S. Mazumder, Eds. Academic Press, 2022, pp. 127–159. [Online]. Available: https://doi.org/10.1016/B978-0-12-818143-0.00012-2

[13] Y. Camaraza-Medina, A. Hernández-Guerrero, and J. L. Luviano-Ortiz, "Experimental study on influence of the temperature and composition in the steels thermo physical properties for heat transfer applications," *Journal of Thermal Analysis and Calorimetry*, vol. 147, no. 21, pp. 11 805–11 821, Nov 2022. [Online]. Available: https://doi.org/10.1007/s10973-022-11410-8

[14] J. Howell, M. Meng"u, K. Daun, and R. Siegel, *Thermal Radiation Heat Transfer*. CRC Press, 2021. [Online]. Available: https://lc.cx/2KIpyY

[15] J. Farmer and S. Roy, "A quasi-Monte Carlo solver for thermal radiation in participating media," *Journal of Quantitative Spectroscopy and Radiative Transfer*, vol. 242, p. 106753, 2020. [Online]. Available: https://doi.org/10.1016/j.jqsrt.2019.106753

[16] T. Li, X. Lin, Y. Yuan, D. Liu, Y. Shuai, and H. Tan, "Effects of flame temperature and radiation properties on infrared light field imaging," *Case Studies in Thermal Engineering*, vol. 36, p. 102215, 2022. [Online]. Available: https://doi.org/10.1016/j.csite.2022.102215

[17] S. Li, Y. Sun, J. Ma, and R. Zhou, "Angular-spatial discontinuous galerkin method for radiative heat transfer with a participating medium in complex three-dimensional geometries," *International Communications in Heat and Mass Transfer*, vol. 145, p. 106836, 2023. [Online]. Available: https://doi.org/10.1016/j.icheatmasstransfer.2023.106836

[18] J. Ávalos Patiño, S. Dargaville, S. Neethling, and M. Piggott, "Impact of inhomogeneous unsteady participating media in a coupled convection–radiation system using finite element based methods," *International Journal of Heat and Mass Transfer*, vol. 176, p. 121452, 2021. [Online]. Available: https://doi.org/10.1016/j.ijheatmasstransfer.2021.121452

[19] Y. Camaraza-Medina, A. Hernández-Guerrero, and J. L. Luviano-Ortiz, "Analytical view factor solution for radiant heat transfer between two arbitrary rectangular surfaces," *Journal of Thermal Analysis and Calorimetry*, vol. 147, no. 24, pp. 14 999–15 016, Dec 2022. [Online]. Available: https://doi.org/10.1007/s10973-022-11646-4

[20] B.-H. Gao, H. Qi, J.-W. Shi, J.-Q. Zhang, Y.-T. Ren, and M.-J. He, "An equation-solving method based on radiation distribution factor for radiative transfer in participating media with diffuse boundaries," *Results in Physics*, vol. 36, p. 105418, 2022. [Online]. Available: https://doi.org/10.1016/j.rinp.2022.105418

[21] S. Sun, "Simultaneous reconstruction of thermal boundary condition and physical properties of participating medium," *International Journal of Thermal Sciences*, vol. 163, p. 106853, 2021. [Online]. Available: https://doi.org/10.1016/j.ijthermalsci.2021.106853

[22] B.-H. Gao, H. Qi, A.-T. Sun, J.-W. Shi, and Y.-T. Ren, "Effective solution of three-dimensional inverse radiation problem in participating medium based on RDFIEM," *International Journal of Thermal Sciences*, vol. 156, p. 106462, 2020. [Online]. Available: https://doi.org/10.1016/j.ijthermalsci.2020.106462

[23] E. Gümücssu and H. I. Tarman, "Numerical simulation of duct flow in the presence of participating media radiation with total energy based entropic lattice Boltzmann method," *International Journal of Thermofluids*, vol. 20, p. 100516, 2023. [Online]. Available: https://doi.org/10.1016/j.ijft.2023.100516

[24] Y. Camaraza-Medina, A. M. Rubio-Gonzales, O. M. Cruz-Fonticiella, and O. F. Garcia-Morales, "Analysis of pressure influence over heat transfer coefficient on air cooled condenser," *Journal Européen des Systèmes Automatisés*, vol. 50, no. 3, pp. 213–226, 2017. [Online]. Available: https://doi.org/10.3166/JESA.50.213-226

[25] P. Sadeghi and A. Safavinejad, "Radiative entropy generation in a gray absorbing, emitting, and scattering planar medium at radiative equilibrium," *Journal of Quantitative Spectroscopy and Radiative Transfer*, vol. 201, pp. 17–29, 2017. [Online]. Available: https://doi.org/10.1016/j.jqsrt.2017.06.023

[26] Y. Wang, A. Sergent, D. Saury, D. Lemonnier, and P. Joubert, "Numerical study of an unsteady confined thermal plume under the influence of gas radiation," *International Journal of Thermal Sciences*, vol. 156, p. 106474, 2020. [Online]. Available: https://doi.org/10.1016/j.ijthermalsci.2020.106474

[27] Y. Camaraza-Medina, Y. Retirado-Mediaceja, A. Hernández-Guerrero, and J. Luis Luviano-Ortiz, "Energy efficiency indicators of the steam boiler in a power plant of Cuba," *Thermal Science and Engineering Progress*, vol. 23, p. 100880, 2021. [Online]. Available: https://doi.org/10.1016/j.tsep.2021.100880

[28] Y. Camaraza-Medina, A. Hernández-Guerrero, and J. L. Luviano-Ortiz, "Contour integration for the view factor calculation between two rectangular surfaces," *Heat Transfer*, vol. 53, no. 1, pp. 225–243, 2024. [Online]. Available: https://doi.org/10.1002/htj.22950

[29] Y. Camaraza-Medina, A. Hernandez-Guerrero, and J. L. Luviano-Ortiz, "Radiant energy exchange through participating media composed of arbitrary concentrations of H_2O, CO_2, and CO," *Heat Transfer*, vol. 53, no. 4, pp. 2073–2094, 2024. [Online]. Available: https://doi.org/10.1002/htj.23026

[30] X. Liu, S. Kelm, M. Kampili, G. V. Kumar, and H.-J. Allelein, "Monte Carlo method with SNBCK nongray gas model for thermal radiation in containment flows," *Nuclear Engineering and Design*, vol. 390, p. 111689, 2022. [Online]. Available: https://doi.org/10.1016/j.nucengdes.2022.111689

[31] Y. Camaraza-Medina, A. Hernández-Guerrero, and J. Luis Luviano-Ortiz, "Contour integration for the exchange of radiant energy between diffuse rectangular geometries," *Thermal Science and Engineering Progress*, vol. 47, p. 102289, 2024. [Online]. Available: https://doi.org/10.1016/j.tsep.2023.102289

[32] A. Mukherjee, V. Chandrakar, and J. R. Senapati, "New correlations for infrared suppression devices having louvered diabatic tubes with surface radiation," *Thermal Science and Engineering Progress*, vol. 44, p. 102011, 2023. [Online]. Available: https://doi.org/10.1016/j.tsep.2023.102011

[33] V. Chandrakar, A. Mukherjee, and J. R. Senapati, "Free convection heat transfer with surface radiation from infrared suppression system and estimation of cooling time," *Thermal Science and Engineering Progress*, vol. 33, p. 101369, 2022. [Online]. Available: https://doi.org/10.1016/j.tsep.2022.101369

[34] F. Asllanaj, S. Contassot-Vivier, G. C. Fraga, F. H. França, and R. J. da Fonseca, "New gas radiation model of high accuracy based on the principle of weighted sum of gray gases," *Journal of Quantitative Spectroscopy and Radiative Transfer*, vol. 315, p. 108887, 2024. [Online]. Available: https://doi.org/10.1016/j.jqsrt.2023.108887

[35] Y. Camaraza-Medina, A. A. Sánchez Escalona, O. Miguel Cruz-Fonticiella, and O. F. García-Morales, "Method for heat transfer calculation on fluid flow in single-phase inside rough pipes," *Thermal Science and Engineering Progress*, vol. 14, p. 100436, 2019. [Online]. Available: https://doi.org/10.1016/j.tsep.2019.100436